Improved Operating Parameters for Hydrogen Peroxide-Generating Gas Diffusion Electrodes

Thorben Muddemann[1,*], Dennis R. Haupt[2], Michael Sievers[2], and Ulrich Kunz[1]

DOI: 10.1002/cite.201900137

Supporting Information available online

The influence of process parameters on the H_2O_2 yield of gas diffusion electrodes (GDE) are investigated. The investigated GDEs consist of Vulcan XC72 carbon black and PTFE on gold-plated nickel wire cloth. An electrolysis cell is used to evaluate the influence of various process parameters, such as temperature, pH value, oxygen pressure and stoichiometric factor, electrolyte flow regime, current density and separator material at steady-state conditions. It is found that the investigated GDE enables current efficiencies greater than 90 % at up to 2 kA m^{-2}, whereby lower electrolyte temperatures and higher pH values contribute to higher H_2O_2 yields above 90 % current efficiency.

Keywords: Electrolysis, Gas diffusion electrode, Hydrogen peroxide, H_2O_2 synthesis

Received: September 11, 2019; *revised:* December 18, 2019; *accepted:* February 10, 2020

1 Introduction

Hydrogen peroxide (H_2O_2) is widely used for oxidation reactions with the advantage to decompose to environmentally friendly and non-toxic products [1]. At present, the industrial production is based on the anthraquinone process [2], but the electrochemical in situ generation of H_2O_2 enables other applications, especially in wastewater treatment [3, 4]. An innovative concept to reduce organic contamination is the combination of a hydroxyl radical generating boron-doped diamond (BDD) anode and a cathodic H_2O_2 producing gas diffusion electrode (H_2O_2-GDE) [5]. Such a double oxidant generating system is not commercially available yet, probably due to commercially unavailable high-yielding H_2O_2-GDEs applicable at higher current densities. Higher current densities are important, especially to minimize the active electrode area and, thus, minimizing the expenses for cost-intensive BDD anodes [6, 7]. High yields are also necessary for an improved economic efficiency of the in situ generation of H_2O_2. At present, only GDEs in small laboratory scales are available [8, 9]. Therefore, a high-yielding H_2O_2-GDE has been developed and its performance is optimized by systematic process parameter variation in this study.

The electrochemical synthesis of H_2O_2 at GDEs is done by the reduction of oxygen and water via the two-electron step (Eqs. (1) and (4)), which is competitive with the four-electron step (Eqs. (2) and (5)) and the electrochemical H_2O_2 reduction (Eq. (3)). H_2O_2 deprotonation (Eq. (6)) and hydrogen evolution (Eq. (7)) form further side reactions [10–13].

$$O_2 + 2H^+ + 2e^- \rightleftharpoons H_2O_2 \quad (E^0 = 0.695\text{V}) \tag{1}$$

$$O_2 + 4H^+ + 4e^- \rightleftharpoons 2H_2O \quad (E^0 = 1.229\text{V}) \tag{2}$$

$$H_2O_2 + 2H^+ + 2e^- \rightleftharpoons 2H_2O \quad (E^0 = 1.776\text{V}) \tag{3}$$

$$O_2 + 2H_2O + 2e^- \rightleftharpoons H_2O_2 + 2OH^- \quad (E^0 = -0.146\text{V}) \tag{4}$$

$$2H_2O + O_2 + 4e^- \rightleftharpoons 4OH^- \quad (E^0 = 0.401\text{V}) \tag{5}$$

$$2H_2O_2 \rightleftharpoons 2H_2O + O_2 \tag{6}$$

$$2H^+ + 2e^- \rightleftharpoons H_2 \quad (E^0 = 0.0\text{V}) \tag{7}$$

The use of carbon materials for the electrochemical H_2O_2 generation was patented in 1931 [14] and nowadays most electrodes for electrochemical synthesis are still based on carbon. It enables the two-electron reaction step, is inexpensive and offers sufficient chemical and thermal stability

[1]Thorben Muddemann, Ulrich Kunz
muddemann@icvt.tu-clausthal.de
Clausthal University of Technology, Institute of Chemical and Electrochemical Process Engineering, Leibnizstraße 17, 38678 Clausthal-Zellerfeld, Germany.

[2]Dennis R. Haupt, Michael Sievers
Clausthal University of Technology, CUTEC Research Center for Environmental Technologies, Leibnizstraße 23, 38678 Clausthal-Zellerfeld, Germany.

[15, 16]. Although carbon has been known as catalyst for nearly one century, the literature mostly focuses on the screening of novel catalysts and combinations [17–20] instead of further optimizing carbon systems through design and operation parameters [21, 22]. Until today, only few studies have examined the influence of the operating parameters of H_2O_2-generating GDE performance according to Tab. S1 and the detailed comparison of published studies given in the Supporting Information.

Even if there is consensus in the literature that higher temperatures promote the self-decomposition of H_2O_2, there is dissent regarding the influence of the pH value, the electrolyte and gaseous flow rates. Furthermore, the impact of the differential pressure of the gas across the GDE has not been evaluated yet.

Therefore, this contribution investigates the impact of numerous process parameters including the differential pressure of gas on the H_2O_2 yield of GDEs. In order to ensure a proper relation of the measured differences in yield to defined operating conditions, the experimental parameter study is investigated at steady state for the first time.

2 Experimental

2.1 Electrodes

The investigated H_2O_2-GDE was developed in cooperation with Covestro AG (Germany) as part of the publicly funded project RADAR [23]. This electrode is already available in technical relevant scales (up to 2.7 m^2). The GDE is a pure carbon electrode (no additional catalyst) consisting of Vulcan XC72 carbon black (60 %; Cabot Corp., USA) and PTFE TF2053Z (40 %, Dyneon GmbH, Germany) on gold-plated nickel wire cloth (Haver & Böcker OHG, Germany).

2.2 Laboratory Electrolysis and Cell Design

The electrolysis cell houses planar electrodes with a geometric area of 100 cm^2 and is shown in simplified form with its material flows in Fig. 1. A Nafion N-438 (Fuel Cell Store, USA) cation exchange membrane separated the anodic compartment from the cathodic one and was placed on the anode in zero-gap arrangement. This anode was a dimensionally stable anode (DSA) based on an expanded metal Ti-electrode with IrO_2 coating (Magneto special anodes B.V., Netherlands) for the oxygen evolution reaction (OER; Eq. (8) and (9)).

$$H_2O \rightleftharpoons 0.5O_2 + 2H^+ + 2e^- \quad (E^0 = 1.229\text{V}) \tag{8}$$

$$2OH^- \rightleftharpoons 0.5O_2 + H_2O + 2e^- \quad (E^0 = 0.401\text{V}) \tag{9}$$

The distance between membrane and GDE was 3 mm. The reaction system reveals an alkalization of the catholyte (proton consumption or hydroxyl ion generation) and an acidification of the anolyte (proton generation or hydroxyl ion consumption). To compensate this pH shift and to achieve steady-state conditions, the system included dosings and overflows at the anodic and cathodic side.

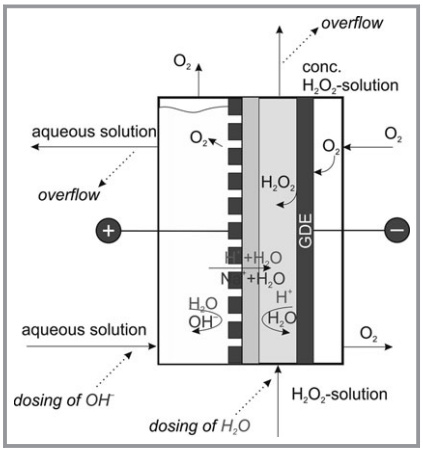

Figure 1. Schematic of the laboratory electrolysis with DSA (+), membrane (gray), GDE (–) and its material flows. Dosings and overflows are marked with dotted lines. Aimed reactions and products are shown (acidic: above; alkaline: below the arrow).

To reach steady-state operation, the electrolysis system was controlled by an embedded system (National Instruments cRio, USA). The GDE backpressure was adjusted by leading the excess oxygen/air from the cathodic side in a water column. The differential pressure was measured directly through a pressure transmitter at the gas outlet of the cell. All experiments were operated in galvanostatic mode. Electrode potentials were measured through Luggin capillaries and reversible hydrogen electrodes (RHE, Gaskatel GmbH, Germany) at two different geometrical points. The electrolytes (anolyte and catholyte each 1 L) were pumped by centrifugal pumps (type MPN 80 and MPN 101, Schmitt GmbH, Germany) and the dosing for steady state was carried out by membrane pumps (Simdos 02, KNF GmbH, Germany). The temperature of the entire system was kept constant by several double-tube heat exchangers (self-made) and a cooling circulator (Huber ministat 230, Germany).

2.3 Analytical Methods

Mass balances were used to determine current efficiencies at steady state. Therefore, the mass flow of dosings, overflows and its concentrations were measured over a defined period. H_2O_2 concentrations were determined by iodometry [24] and the H_2O_2 current efficiencies were calculated by Eq. (10):

$$C.E. = \frac{z\,F\,w_{H_2O_2}\Delta\left(\dot{m}_{\text{start/end}}\right)}{M_{H_2O_2}\,j\,A} \cdot 100 \tag{10}$$

With z as the stoichiometric number of transferred electrons (2), F as Faraday constant (96 485.33 C mol^{-1}), $w_{H_2O_2}$ (g g^{-1}) as H_2O_2 concentration, $\Delta\dot{m}_{start/end}$ (g s^{-1}) as the catholyte overflow rate, $M_{H_2O_2}$ (g mol^{-1}) as molar mass of H_2O_2, j (kA m^{-2}) for the current density and A (m^2) for the geometric electrode area. The hydroxyl ion/proton concentrations were determined via acid-base titration. To determine reliable yields including error estimation, each analysis was carried out three times to determine the average value and its standard deviation of the current yield.

2.4 Chemicals

The GDEs were operated with oxygen (3.5 N, Linde AG, Germany) and synthetic air (20 % O_2 and 80 % N_2). Deionized water (behropur, Behr Labor-Technik GmbH, Germany), caustic soda (No. 9356.2, Carl Roth GmbH + Co. KG, Germany), sodium sulfate (No. 0966.2, Roth) and sulphuric acid (No. 9316.2, Roth) were used for preparation of the electrolytes. The chemicals for the titration were purchased from Roth: sodium thiosulfate solution (No. K022.1), ammonium heptamolybdate tetrahydrate (No. 7311.1) and potassium iodide (No. 6750.3).

3 Results and Discussion: Influence of the Process Parameters on H_2O_2 Current Efficiency

The results of the successive process parameter variation are presented below. Since the investigated GDE should be used in wastewater treatment, higher current densities are favorable, and the lowest relevant current density was set to 0.5 kA m^{-2}.

3.1 Temperature Influence

To investigate the influence of temperature, the dosing of the laboratory system was adjusted to achieve a concentration of 1 M NaOH in the anolyte and catholyte. For this purpose, both circuits were filled with 1 M NaOH at startup of the plant and 1.5 M NaOH was added to the anolyte (approx. 319 g h^{-1}) and demineralized water to the catholyte (approx. 171 g h^{-1}) during electrolysis. The current density was set to 0.5 kA m^{-2} with an oxygen stoichiometric factor of 3.6 and a gaseous pressure difference of 35 mbar. This resulted in a NaOH concentration in the catholyte of 0.979 ± 0.019 M after reaching steady-state condition. The influence of the temperature is shown in Fig. 2, indicating that lower temperatures lead to higher cell voltages due to lower conductivities, but also to the highest yields. Current efficiencies for H_2O_2 production of greater 90 % were measured at 15 °C with following process parameters: An oxygen stoichiometric factor of 3.6, a differential pressure of

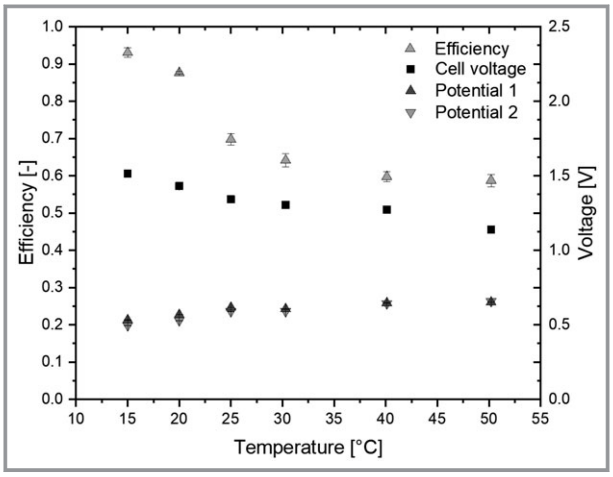

Figure 2. Influence of temperature on H_2O_2 yield at 0.5 kA m^{-2}, oxygen stoichiometric factor of 3.6, differential pressure of 35 mbar and 1 M NaOH.

35 mbar and an electrolyte flow rate of 33 L h^{-1} (turbulent flow regime). At higher temperatures, a decrease in H_2O_2 yield was found by lower H_2O_2 concentrations measured in the overflow outlet of the system, starting from 15 °C (1.541 ± 0.034 wt %), to 20 °C (1.437 ± 0.005 wt %), 25 °C (1.207 ± 0.028 wt %), 30 °C (1.038 ± 0.029 wt %), 40 °C (0.985 ± 0.025 wt %) and 50 °C (0.637 ± 0.032 wt %).

The determined current yield for hydroxide ions, which are formed in the alkaline environment as a by-product of the H_2O_2 formation, indicate current efficiencies of greater than 90 % for all experiments. It is probable that H_2O_2 was formed with higher yields even at high temperatures but due to an expected increase of reactivity and self-accelerated decomposition rate at higher temperatures this could not be measured in the experiments. During the experiments with an electrolyte temperature of 50 °C, the electrolyte penetrates through the GDE. Due to the decreasing electrolyte viscosity, a differential pressure of 35 mbar in the gas compartment was no longer sufficient to prevent electrolyte penetration. Up to 40 °C the GDE was operated satisfactorily.

In all experiments, the potential measurements show differences between the two measuring points of up to 40 mV. The large electrode surface area and broad pore size distribution lead to locally different electrode characteristics. Furthermore, oxygen bubbles can be forced through the electrode and cause potential jumps during detachment, which are reflected in the standard deviations. Such observations have already been published for other carbon-based systems [25]. Therefore, besides the local potentials, the integral cell voltage is an important value for electrode performance screening.

3.2 Influence of pH Value

To evaluate the influence of the pH value on the H_2O_2 yield, the dosage mass flow rate of all liquids was kept constant, but the pH value of the added solution (to the catholyte) was varied. Demineralized water was used as dosing agent for the experiment at pH 14 and the catholyte dosing was adjusted to more acidic level (H_2SO_4) for the other operating points.

The investigations show that H_2O_2 has the highest stability at pH 14 and the yield drops rapidly and almost in linear proportion with decreasing pH (Fig. 3). The yield decreased from initially approx. 95 % at pH 14 to 19.3 % at pH 1. The concentration of the H_2O_2 solution changed from 1.6 wt % (pH 14) to 0.34 wt % (pH 1). These yield losses are also due to increasing chemical potentials and reactivity and, thus, self-decomposition of H_2O_2 with decreasing pH value. In alkaline solutions H_2O_2 predominantly exists as HO_2^- and inhibits the self-decomposition at higher pH values [26].

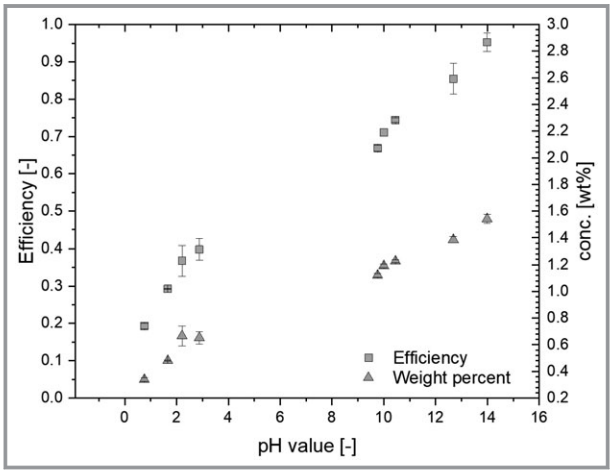

Figure 3. Effect of the pH value on the H_2O_2 yield and concentration. All measurements were done at 0.5 kA m^{-2}, differential pressure of 35 mbar; oxygen stoichiometric factor of 3.6 and 15 °C.

For an in situ wastewater treatment, an acidic pH value adjustment is sometimes used (e.g., for Fenton reaction), but an electrochemical H_2O_2 generator based on carbon GDE should be operated in the alkaline pH range. The combined formation of H_2O_2 and OH^- at alkaline condition is described as negative property in comparison to the stand-alone H_2O_2 formation in acidic condition in literature (Eq. (1)) [27]. However, the test series show that this is an ideal combination since the stabilizing agent is generated in situ at the same reaction step. This result is beneficial since different industrial process waters as well as wastewater streams are highly alkaline [28] and, e.g., H_2O_2 is preferably used in combination with sodium hydroxide in the pulp and paper industry [29].

3.3 Influence of the Flow Regime

A turbulent flow occurs in a plane gap within an electrochemical reactor at Reynolds (*Re*) numbers of greater 2200 to 3600 [30]. In order to investigate the influence of the flow regime, the H_2O_2 yield was determined at 20 L h^{-1} and 33 L h^{-1}, each at different temperatures, but on the same steady-state operation as described above. The *Re* numbers were calculated according to [30] to 1626 (15 °C), 1845 (20 °C) and 1991 (30 °C) for the test series with the laminar catholytic volume flow rate of 20 L h^{-1} and to 2683 (15 °C), 3043 (20 °C) and 3286 (30 °C) for the turbulent flow at 33 L h^{-1}. The anolyte volume flow rate was set at 60 L h^{-1} in all experiments.

The influence of the catholyte flow regime on the H_2O_2 yield is given in Fig. 4. Both the laminar flow (20 L h^{-1}) and the turbulent flow (33 L h^{-1}) show similar results in the considered operating area (1 M NaOH, 0.5 kA m^{-2}) and no significant difference in yield as well as cell voltages can be determined at all temperatures. It should be noted that laminar flow led to higher fluctuations in the H_2O_2 concentration measurement due to a more inhomogeneous mixing at a lower electrode overflow velocity.

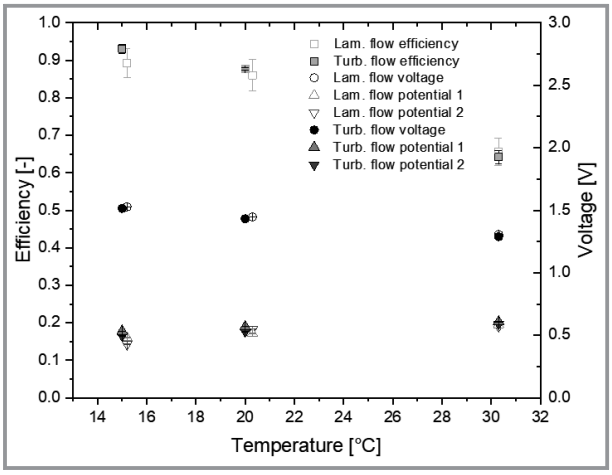

Figure 4. Influence of the flow regime regarding the H_2O_2 yield at 0.5 kA m^{-2}, oxygen stoichiometric factor of 3.6 and a differential pressure of 35 mbar.

3.4 Differential Pressure in the Gas Compartment

Based on the baseline operating point of this study (0.5 kA m^{-2}, 1 M NaOH, 15 °C), further process optimizations were investigated. Varying differential pressures across the GDE do not lead to a significant increase in the H_2O_2 yield, but an increasing pressure leads to a decreasing cell voltage (Fig. 5). An increasing cathode potential causes this cell voltage reduction. Higher backpressures probably push the three-phase boundary layer inside the GDE more toward the liquid phase. Therefore, the voltage drop due to the electrical conductivity of the electrolyte inside the GDE

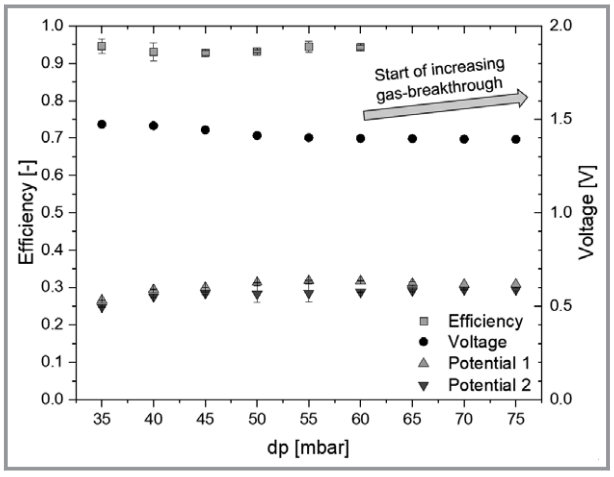

Figure 5. Influence of the differential pressure (*dp*) on H_2O_2 current efficiency, cell voltage and potentials at 0.5 kA m^{-2} and 1 M NaOH.

is reduced. By increasing the pressure from 35 mbar to 55 mbar, more than 70 mV in cell voltage is savable. As a pressure above 60 mbar leads to gas breakthrough from the gas side to the electrolyte side of the GDE, a differential pressure of 55 mbar is recommended for future investigations with this electrode.

3.5 Oxygen Stoichiometric Factor, Air and Separator Material

For economical wastewater treatment, water reuse and water disinfection, a cost-effective H_2O_2 generation is necessary to support economic applications. Therefore, the influence of oxygen stoichiometric factor and the use of air instead of pure oxygen (technical grade) were investigated. Furthermore, the operation with a diaphragm (Zirfon, Agfa-Gevaert N.V., Belgium) as a more cost-effective separator material was compared to the Nafion N-438 cation exchange membrane (CEM), as given in Fig. 6. The operation with an oxygen stoichiometric factor of 1.8 and 3.6 did not show any significant differences regarding the cell voltage (see "CEM; 1.8nO_2, 50 mbar" vs. "CEM; 3.6n O_2; 50 mbar") or only a small difference in H_2O_2 yield (90.09 % ± 0.68 % in comparison to 93.17 % ± 0.42 %). In contrast to this, an operation with air instead of technical O_2 (see "CEM; 3.6nO_2; 35 mbar" to "CEM; 3.6nAir; 35 mbar") led to an increased cell voltage of 540 mV caused by a lower cathode potential. Although the operation with air led to an increased voltage, the efficiency remains constant considering the error bars.

An operation with the CEM led to high yields and excellent separation of anolyte and catholyte without a H_2O_2 crossover flow, because H_2O_2 was not detected in the anolyte. Zirfon was selected as an alternative separator material for cheaper operation (see "CEM; 3.6nO_2; 35 mbar" vs. "Zirfon; 3.6nO_2; 35 mbar"), but it led to a drastic efficiency

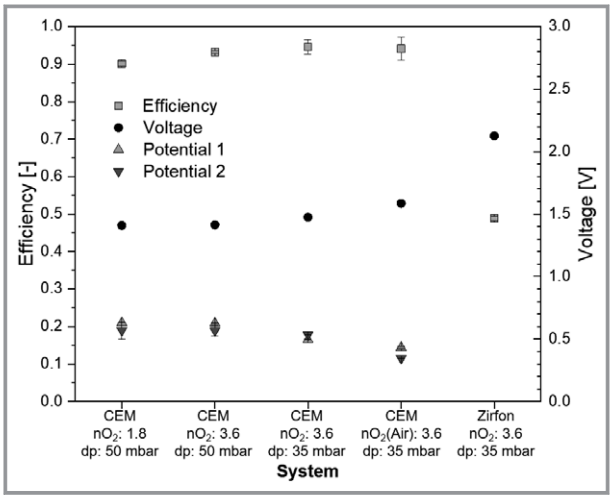

Figure 6. Influence of oxygen stoichiometric ratio (nO_2), air and the separator material on the H_2O_2 current efficiency. Cell voltage and potentials at 0.5 kA m^{-2}, oxygen stoichiometric factor (nO_2) and differential pressure (*dp*) are specified in the legend.

decrease (30–40 %) and the yield dropped to 48.86 % ± 0.53 % (61.06 % incl. H_2O_2 in the anolyte) in combination with an increasing cell voltage of 650 mV. The unspecific ion/molecule separation of a diaphragm like Zirfon is not beneficial for this application.

3.6 Influence of Current Density

Fig. 7 illustrates the influence of the current density on the H_2O_2 yield. The volume flow rates of liquid dosings (and overflows) were controlled in relation of the current to reach steady state with 1 M NaOH despite the higher faradaic formation rates at higher current densities. This

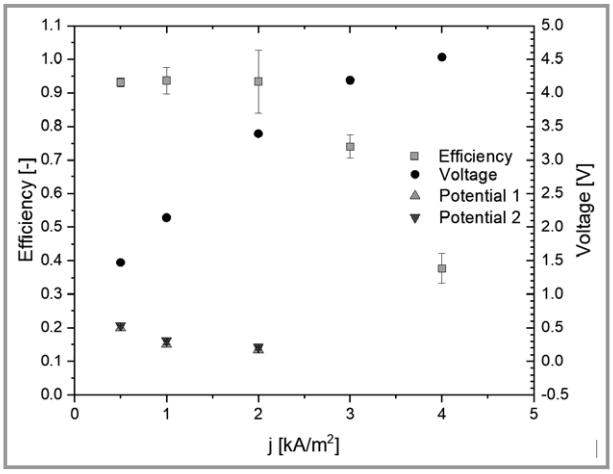

Figure 7. Influence of current density to the H_2O_2 current efficiency, cell voltage and potentials at 1 M NaOH, 15 °C and a differential pressure of 35 mbar at an oxygen stoichiometric factor of 3.6.

enables a suitable comparison through identical pH values even across different current densities.

The data indicate that yields of more than 90 % were also reached in the higher current density range of up to 2 kA m^{-2}. Due to the high cathodic potential at 2 kA m^{-2}, the operation at 3 kA m^{-2} and 4 kA m^{-2} was also investigated. Both current densities led to lower efficiencies and an electrolyte breakthrough through the GDE occurred during each experiment. Due to strong potential fluctuations through the electrolyte breakthrough, the potentials of these operating points are omitted. After disassembling the test cell, a partially swollen electrode material was visible in both cases.

The GDEs of the 3 kA m^{-2} and 4 kA m^{-2} test series and the intact one after the 0.5 kA m^{-2} experiment were examined by SEM images. Fig. 8-1 shows the cross section of an intact H_2O_2-GDE, including its nickel wire cloth. Fig. 8-2 shows such a transition from an almost intact GDE surface of the 4 kA m^{-2} GDE (left) to a swollen surface (right). For further illustration, the swollen state of the GDE after 3 kA m^{-2} is shown in Fig. 8-3 and after 4 kA m^{-2} in Fig. 8-4. The swelling is probably caused by oxygen evolution through H_2O_2 decomposition, which might occur at the higher current densities through mass transfer limitation of the product at the inner electrode or through hydrogen evolution. Swelling and cracking occurrence increase strongly through the H_2O_2 generation rates at current densities above 2 kA m^{-2}. Nevertheless, the investigated H_2O_2-GDE was stable up to 2 kA m^{-2} and clearly surpasses most of the GDEs mentioned in the literature.

4 Conclusions

A process parameter study was performed to optimize the efficiency of H_2O_2-generating gas diffusion electrodes. This study includes the process parameters temperature, pH value, oxygen pressure and oxygen stoichiometric factor, electrolyte flow regime, current density and separator material. A laboratory reactor was operated at steady-state conditions for a fair and accurate comparison and evaluation of process parameters. This approach was selected due to the contradictory results reported in literature, mainly caused by changing pH values.

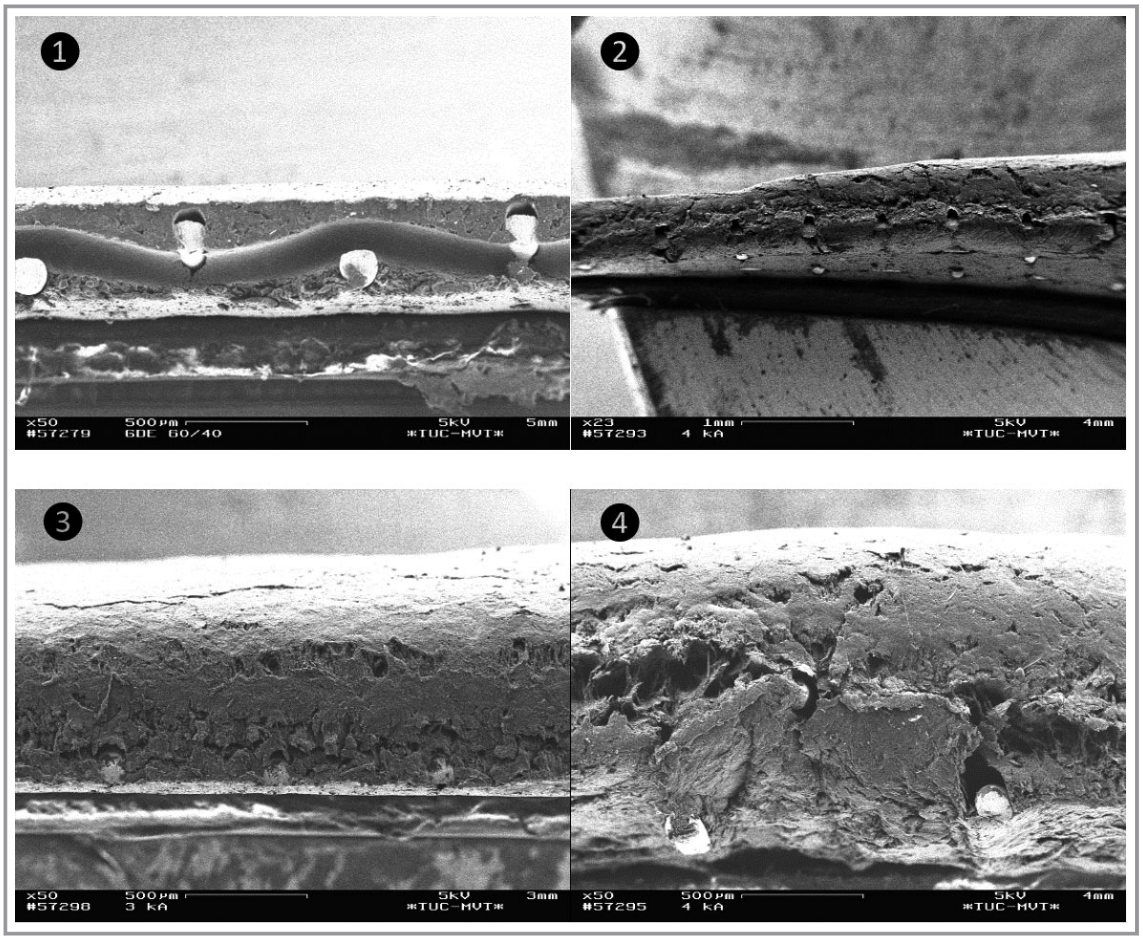

Figure 8. SEM images of the H_2O_2-GDE after different current density loadings: an intact GDE surface after 2 kA m^{-2} current load (1), defective GDE surface after 3 kA m^{-2} (3) and after 4 kA m^{-2} load (2 and 4).

The investigations clearly show that especially higher temperatures and lower pH values decrease the H_2O_2 yield probably due to H_2O_2 decomposition. The present carbon-based GDE enables current yields greater than 90 % at 15 °C and pH 14 at 0.5 kA m^{-2} up to 2 kA m^{-2}. The combined formation of H_2O_2 and OH^- in the alkaline environment is an ideal combination since the stabilizing agent is generated simultaneously, which is a great advantage of electrochemical H_2O_2 formation. While the temperature and pH value of the electrolyte have a significant influence on the H_2O_2 yield, no significant difference is observed between laminar and turbulent electrolyte flow regimes.

Furthermore, the cell voltage can be reduced by selecting a decent oxygen pressure difference in the gas compartment. A differential pressure slightly lower than the gas breakthrough pressure of the GDE resulted in a cell voltage reduction of more than 70 mV. In contrast, the operation with 1.8-fold or 3.6-fold oxygen stoichiometric factor did not show a significant difference in the cell voltage. Therefore, an operation with 1.8-fold oxygen is recommended. With the present GDE, an operation with air as gas is also possible, because similar H_2O_2 yields are found compared to the operation with technical grade oxygen. However, it led to an increase in cell voltage and, therefore, more electric power generation is necessary.

The investigations show that pure carbon-based GDEs enable high yields of H_2O_2 above 90 % current efficiency in alkaline medium.

A H_2O_2 concentration of 1.6 wt % at a production rate of 1.86 mol $h^{-1}m^{-2}A^{-1}$ can be reached. In addition, the impact of process parameters on the efficiency of the electrolysis should generally receive more attention due to their possibly more important influence compared to catalyst type and composition.

Supporting Information

Supporting Information for this article can be found under DOI: https://doi.org/10.1002/cite.201900137. This section includes additional references to primary literature relevant for this research [31–39].

The authors thank Federal Ministry of Education and Research (Bundesministerium für Bildung und Forschung), BMBF, Germany, for funding this study (contract number 03XP0107). Many thanks also to Covestro AG for providing the GDEs.

Symbols used

A	[m^2]	area
$C.E.$	[–]	current efficiency
F	[C mol^{-1}]	Faraday constant, 96 485.33
j	[kA m^{-2}]	current density
$M_{H_2O_2}$	[g mol^{-1}]	molar mass of H_2O_2
$\Delta\dot{m}_{start/end}$	[g s^{-1}]	catholyte overflow rate
$nAir$	[–]	air stoichiometric factor
nO_2	[–]	oxygen stoichiometric factor
$w_{H_2O_2}$	[g g^{-1}]	H_2O_2 concentration
z	[–]	stoichiometric number of transferred electrons

Abbreviations

BDD	boron doped diamond
CEM	cation exchange membrane
DSA	dimensionally stable anode
GDE	gas diffusion electrode
H_2O_2-GDE	hydrogen peroxide-generating gas diffusion electrode
RHE	reversible hydrogen electrode

References

[1] M. Giomo, A. Buso, P. Fier, G. Sandonà, B. Boye, G. Farnia, *Electrochim. Acta* **2008**, *54 (2)*, 808–815. DOI: https://doi.org/10.1016/j.electacta.2008.06.038
[2] J. M. Campos-Martin, G. Blanco-Brieva, J. L. G. Fierro, *Angew. Chem., Int. Ed.* **2006**, *45 (42)*, 6962–6984. DOI: https://doi.org/10.1002/anie.200503779
[3] F. C. Moreira, R. A. R. Boaventura, E. Brillas, V. J. P. Vilar, *Appl. Catal., B* **2017**, *202*, 217–261. DOI: https://doi.org/10.1016/j.apcatb.2016.08.037
[4] H. Särkkä, A. Bhatnagar, M. Sillanpää, *J. Electroanal. Chem.* **2015**, *754*, 46–56. DOI: https://doi.org/10.1016/j.jelechem.2015.06.016
[5] D. Haupt, T. Muddemann, U. Kunz, M. Sievers, *Electrochem. Commun.* **2019**, *101*, 115–119. DOI: https://doi.org/10.1016/j.elecom.2019.02.020
[6] J. Radjenovic, D. L. Sedlak, *Environ. Sci. Technol.* **2015**, *49 (19)*, 11292–11302. DOI: https://doi.org/10.1021/acs.est.5b02414
[7] H. Barndok, D. Hermosilla, C. Negro, A. M. Blanco, *ACS Sustainable Chem. Eng.* **2018**, *6 (5)*, 5888–5894. DOI: https://doi.org/10.1021/acssuschemeng.7b04234
[8] M. Panizza, G. Cerisola, *Electrochim. Acta* **2008**, *54 (2)*, 876–878. DOI: https://doi.org/10.1016/j.electacta.2008.07.063
[9] G. Agladze, P. Nikoleishvili, V. Kveselava, G. Tsurtsumia, G. Gorelishvili, D. Gogoli, I. Kakhniashvili, *J. Power Sources* **2012**, *218*, 46–51. DOI: https://doi.org/10.1016/j.jpowsour.2012.06.086
[10] W. H. Rankin, D. R. Lide, *CRC Handbook of Chemistry and Physics*, 89th ed., Vol. 15, CRC Press, Boca Raton, FL **2009**.
[11] Y. L. Zheng, D. Mei, Y.-X. Chen, S. Ye, *Electrochem. Commun.* **2014**, *39*, 19–21. DOI: https://doi.org/10.1016/j.elecom.2013.12.005
[12] E. Yeager, *Electrochim. Acta* **1984**, *29 (11)*, 1527–1537.
[13] *Comprehensive Treatise of Electrochemistry, Kinetics and Mechanisms of Electrode Processes*, Volume 7 (Eds: B. E. Conway et al.), Springer US, New York **1983**.
[14] E. Berl, *Patent US2000815A*, **1935**.
[15] M. H. M. T. Assumpção, R. F. B. de Souza, D. C. Rascio, J. C. M. Silva, M. L. Calegaro, I. Gaubeur, T. R. L. C. Paixão, P. Hammer, M. R. V. Lanza, M. C. Santos, *Carbon* **2011**, *49 (8)*, 2842–2851. DOI: https://doi.org/10.1016/j.carbon.2011.03.014

[16] G. V. Kornienko, N. V. Chaenko, I. S. Vasil'eva, G. A. Kolyagin, V. L. Kornienko, *Russ. J. Appl. Chem.* **2010**, *83 (2)*, 253–257. DOI: https://doi.org/10.1134/S1070427210020126
[17] J. F. Carneiro, R. S. Rocha, P. Hammer, R. Bertazzoli, M. R. V. Lanza, *Appl. Catal., A* **2016**, *517*, 161–167. DOI: https://doi.org/10.1016/j.apcata.2016.03.013
[18] E. Lobyntseva, T. Kallio, N. Alexeyeva, K. Tammeveski, K. Kontturi, *Electrochim. Acta* **2007**, *52 (25)*, 7262–7269. DOI: https://doi.org/10.1016/j.electacta.2007.05.076
[19] U. A. Paulus, T. J. Schmidt, H. A. Gasteiger, R. J. Behm, *J. Electroanal. Chem.* **2001**, *495*, 134–145.
[20] F. L. Silva, R. M. Reis, W. R. P. Barros, R. S. Rocha, M. R. V. Lanza, *J. Electroanal. Chem.* **2014**, *722–723*, 32–37. DOI: https://doi.org/10.1016/j.jelechem.2014.03.007
[21] H. Luo, C. Li, C. Wu, X. Dong, *RSC Adv.* **2015**, *5 (80)*, 65227–65235. DOI: https://doi.org/10.1039/C5RA09636G
[22] F. C. Moreira, R. A. R. Boaventura, E. Brillas, V. J. P. Vilar, *Appl. Catal., B* **2017**, *202*, 217–261. DOI: https://doi.org/10.1016/j.apcatb.2016.08.037
[23] *RADAR: Wastewater Treatment by OH-Radicals*, DECHEMA e.V., Frankfurt **2017**. www.machwas-material.de/en/RADAR.html
[24] G. Hilt, P. Rinze, *Chemisches Praktikum für Mediziner*, Springer Fachmedien, Wiesbaden **2015**.
[25] A. Köppen, *Kohlenstoffbasierte Sauerstoffverzehrkathoden für die Chlor-Alkali-Elektrolyse*, Verlag Dr. Hut, München **2017**.
[26] G. R. Agladze, G. S. Tsurtsumia, B.-I. Jung, J.-S. Kim, G. Gorelishvili, *J. Appl. Electrochem.* **2007**, *37 (3)*, 375–383. DOI: https://doi.org/10.1007/s10800-006-9269-x
[27] H. U. Suess, *Pulp Bleaching Today*, Walter de Gruyter, Berlin **2010**.
[28] A. Bulan, R. Weber, T. Muddemann, *Patent WO2018/029200A1*, **2018**.
[29] P. C. Foller, R. T. Bombard, *J. Appl. Electrochem.* **1995**, *25 (7)*, 613–627. DOI: https://doi.org/10.1007/BF00241923
[30] V. M. Schmidt, *Elektrochemische Verfahrenstechnik*, Wiley-VCH, Weinheim **2003**.
[31] G. A. Kolyagin, V. L. Kornienko, *Russ. J. Appl. Chem.* **2003**, *7*, 1070–1075.
[32] I. Salmerón, K. V. Plakas, I. Sirés, I. Oller, M. I. Maldonado, A. J. Karabelas, S. Malato, *Appl. Catal., B* **2019**, *242*, 327–336. DOI: https://doi.org/10.1016/j.apcatb.2018.09.045
[33] C. Flox, J. A. Garrido, R. M. Rodríguez, P.-L. Cabot, F. Centellas, C. Arias, E. Brillas, *Catal. Today* **2007**, *129 (1–2)*, 29–36. DOI: https://doi.org/10.1016/j.cattod.2007.06.049
[34] G. R. Agladze, G. S. Tsurtsumia, B.-I. Jung, J.-S. Kim, G. Gorelishvili, *J. Appl. Electrochem.* **2007**, *37 (9)*, 985–990. DOI: https://doi.org/10.1007/s10800-007-9325-1
[35] G. R. Agladze, G. S. Tsurtsumia, B.-I. Jung, J.-S. Kim, G. Gorelishvili, *J. Appl. Electrochem.* **2007**, *37 (3)*, 385–393. DOI: https://doi.org/10.1007/s10800-006-9268-y
[36] Y. Lu, G. Liu, H. Luo, R. Zhang, *Electrochim. Acta* **2017**, *248*, 29–36. DOI: https://doi.org/10.1016/j.electacta.2017.07.085
[37] M. S. Saha, A. Denggerile, Y. Nishiki, T. Furuta, T. Ohsaka, *Electrochem. Commun.* **2003**, *5 (6)*, 445–448. DOI: https://doi.org/10.1016/S1388-2481(03)00097-3
[38] T. Pérez, G. Coria, I. Sirés, J. L. Nava, A. R. Uribe, *J. Electroanal. Chem.* **2018**, *812*, 54–58. DOI: https://doi.org/10.1016/j.jelechem.2018.01.054
[39] L. Li, H. Hu, X. Teng, Y. Yu, Y. Zhu, X. Su, *Chem. Eng. Process.* **2018**, *133*, 34–39. DOI: https://doi.org/10.1016/j.cep.2018.09.013

